

# Parameter-free renormalization group theory of the order-disorder phase transition in $\beta$ -brass

V I Tokar

*Université de Strasbourg, CNRS, IPCMS, UMR 7504, F-67000 Strasbourg, France*

<sup>1</sup>*G. V. Kurdyumov Institute for Metal Physics of the N.A.S. of Ukraine, 36 Acad. Vernadsky Boulevard, UA-03142 Kyiv, Ukraine*

---

## Abstract

A self-consistent (SC) renormalization group approach analogous to the coherent potential approximation (CPA) in the band structure theory of disordered alloys has been developed. With the use of generalized CPA techniques a renormalization group equation in the local potential approximation (LPA) derived previously for spatially homogeneous systems has been extended to the lattice case and supplemented with a CPA-like self-consistency condition. To validate the approach it has been applied to the simple cubic Ising model and good agreement of the spontaneous magnetization calculated with the use of the SC-LPA equation with the available exact Monte Carlo simulations data has been established. Then the approach has been applied to the bcc Ising model corresponding to  $\beta$ -brass. With the use of the effective pair interaction values from available *ab initio* calculations the critical temperature, the correlation length and the long range order parameter in the vicinity of the critical point have been calculated in excellent agreement with experimental data. Quantitative arguments have been given in support of the suggestion that the experimentally observed large decrease of the effective critical exponent of the order parameter in comparison with its universal value is enhanced by the positive value of the second neighbour pair interaction found in the *ab initio* calculations.

*Keywords:* self-consistent renormalization group, local potential approximation, ordering in the Ising model, ordering in beta brass, critical temperatures, effective critical exponents of the order parameter

---

## 1. Introduction

Modern theory of binary alloys aims at describing the order-disorder phase transitions fully *ab initio* without resort to any phenomenological input. But

---

*Email address:* tokar@ipcms.unistra.fr (V I Tokar)

<sup>1</sup>Permanent address.

because inclusion of correlated disorder in the band structure calculations meets with serious difficulties [1, 2], theoretical treatment of interatomic correlations at finite temperature is usually separated in two stages. At the first stage the configuration-dependent electronic structure energy is mapped onto the Ising model (IM) with the effective cluster interactions between the spins and at the second stage the IM statistics is treated by means of statistical mechanics [3, 4]. Currently no universal techniques efficient in the calculations at both stages exist because different alloys may exhibit qualitatively different behaviour and a technique efficient in alloys of one kind performs poorly in alloys of different kind. In particular, cluster methods that proved to be quite efficient in the description of the first order phase transitions fail to describe continuous transitions because finite clusters cannot properly account for the long range correlations [3, 5, 6].

The aim of the present paper is to derive a renormalization group (RG) equation based on the self-consistent (SC) functional formalism developed in [7, 5, 6] which proved to be successful in the description of the first order phase transitions. An advantage of such an approach is that it should make possible the treatment of phase transitions of any kind within the same general formalism [8]. The consideration in the present paper will be restricted to models with only the effective pair interactions because in this case the RG approach can be made fully self-contained. For the treatment of higher cluster interactions the cluster techniques would be needed [8].

Though electronic structure calculations will not be discussed in this paper, frequent references to the coherent potential approximation (CPA) [1, 9] will be made as to a generic example of a successful self-consistent (SC) effective-medium theory of the kind we intend to develop. It is widely believed that one of the cause underlying the CPA success lies in its SC nature which was the main motivation for introducing it into the RG theory. Similar to the CPA which assumes that with the site-local disordered potential the multiple scattering of electrons is dominated by the local scattering, the SC RG equation we are going to derive will be based on the local potential approximation (LPA) (see [11, 31] and bibliography therein) and on the self-consistency condition analogous to that used in the CPA.

A major difficulty hampering broader adoption of the LPA equations of the type we are going to use in the present paper [10] is that they belong to the category of non-perturbative RG equations which are currently impossible to rigorously substantiate beyond the perturbation theory or the limit of small Fourier momenta [21, 11, 12, 31]. In this respect they are similar to CPA which also can be rigorously justified only in some limiting cases. However, CPA is being widely used in electronic structure calculations because its soundness has been confirmed by good agreement with the exact Monte Carlo (MC) simulations and with experiment [1, 13, 14]. Because the non-perturbative RG equations are hardly simpler than the equations for the Green's function of disordered alloy, by analogy with the CPA, the SC-LPA equation will be validated in the present paper by comparing its prediction with reliable solutions of the IM [15, 16, 17] and with the experiments on the order-disorder phase transition in  $\beta$ -brass [18].

The pair interaction parameters of the equiatomic Cu-Zn alloy (or  $\beta$ -brass) will be taken from the *ab initio* CPA calculations in [19] which will make our RG description devoid of any phenomenological input. It is hoped that the formal analogy with the CPA and the good agreement of the SC-LPA with known results obtained in [22, 20] and in the present paper will stimulate further investigation of the LPA-based SC RG approach and will ultimately promote it to the status in the alloy thermodynamics similar to the status of CPA in the electronic structure theory.

## 2. Formalism

In the IM formalism the configuration-dependent contribution to the total energy of an equiatomic binary alloy reads [3, 19]

$$E_{conf} = \frac{1}{8} \sum_{ij} V_{ij} s_i s_j \quad (1)$$

where  $s_i = \pm 1$  are the Ising spins occupying  $N$  lattice sites  $i$  and  $V_{ij}$  are the effective pair interactions which following [19, 18] we will restrict to only the nearest neighbour (nn) ( $V_1$ ) and the second neighbour ( $V_2$ ) interactions which is sufficient for the discussion of ordering in  $\beta$ -brass [16, 19, 18]. In (1) linear in  $s_i$  terms are absent because the transformation  $s_i \rightarrow -s_i$  corresponds to replacement of atoms of one kind by the atoms of another kind and in the equiatomic alloy this should not change the configurational energy. In the IM language this means that the external magnetic field is equal to zero. On bipartite lattices, such as the simple cubic (sc) and the bcc lattices, this additionally makes possible to switch the signs of spins  $s_i \rightarrow -s_i$  on one of the two interpenetrating sublattices and simultaneously reverse the signs of  $V_{ij}$  connecting spins at different sublattices to arrive at a model with the same statistical properties but with different order parameter [16]. In the case under consideration the antiferromagnetic order will change to the ferromagnetic (FM) one and because the FM order is simpler, in the study of ordering in  $\beta$ -brass (bcc lattice) we will deal with the transformed system. To avoid confusion,  $V_1$  and  $V_2$  will retain their physical values while in explicit calculations we will use the reduced (i.e., divided by  $k_B T$ ) Hamiltonian of the form

$$H_I = \frac{1}{2} \sum_{ij} \epsilon_{ij} s_i s_j - \sum_i h_i s_i + N \epsilon_0 / 2 \quad (2)$$

with the interactions between the nn and the second neighbour spins  $\epsilon_1 = -V_1/4k_B T$  (note the sign reversal) and  $\epsilon_2 = V_2/4k_B T$ , respectively. Besides, we introduced into  $\epsilon_{ij}$  a diagonal part  $-\epsilon_0 \delta_{ij}$  with

$$\epsilon_0 = \frac{-8V_1 + 6V_2}{4k_B T} \quad (3)$$

which is compensated by the last term in (2)) because of the identity  $s_i^2 = 1$ . This is done to ensure the quadratic behaviour of the Fourier-transformed  $\epsilon$  at small momenta [16]

$$\epsilon(\mathbf{k})|_{\mathbf{k} \rightarrow 0} \simeq \frac{V_1 - V_2}{k_B T} a^2 \mathbf{k}^2 \quad (4)$$

where  $a$  in the bcc case was chosen to be equal to one half of the length of the cube edge so that the vectors connecting nn sites have coordinates  $(\pm a, \pm a, \pm a)$  and their length  $a_1 = \sqrt{3}a$  (in the sc case the cube edge and the nn distance coincide).

Besides, in (2) we added the linear coupling of spins to the source field  $h$  that will be needed, e.g., in the formulation of the self-consistency condition. At the end of the calculations, however, it will be set equal to zero because only the equiatomic alloys and the IM in zero external field will be studied in the present paper.

The calculations below will be based on the general effective medium approach introduced in [7] that generalizes CPA on a broad class of field-theoretic models. Because the formalism was recapitulated in several papers (see, e.g., [5, 6, 20]) only its one-component variant sufficient for IM will be briefly explained below.

In the functional-integral representation the partition function of the Ising model (2) reads

$$Z[h] = e^{N\epsilon_0/2} \prod_l \int ds_l 2\delta(s_l^2 - 1) e^{-\frac{1}{2} \sum_{ij} \epsilon_{ij} s_i s_j + \sum_i h_i s_i} \quad (5)$$

where the delta functions fix the continuous spins  $s_i$  to their Ising values  $\pm 1$ . By standard manipulations [7, 5, 6, 20] (5) can be cast in the form (see, e.g., equations (5) and (6) in [7])

$$Z[h] = \exp\left(\frac{1}{2} h G h\right) R[Gh] \quad (6)$$

where the vector-matrix notation has been used in the  $N$ -dimensional space of the lattice sites so that, e.g.,  $Gh = \sum_j G_{ij} h_j$ , etc. The propagator matrix  $G$  is translationally-invariant and its Fourier transform reads

$$G(\mathbf{k}) = \frac{1}{\epsilon(\mathbf{k}) + r}. \quad (7)$$

Here momentum-independent constant  $r$  plays the role of the SC self-energy both in the single-site cluster approximations [7, 5, 6, 20] and in the CPA [9]. In the IM case it can be introduced into (5) in the same manner as  $\epsilon_0$  in (2) with the corresponding compensating term accounted for in (6) through

$$\begin{aligned} R[s] &= \det(2\pi G)^{1/2} e^{N(r-\epsilon_0)/2} \exp\left(\frac{\partial}{\partial s} G \frac{\partial}{\partial s}\right) \prod_l [2\delta(s_l^2 - 1)] \\ &= \exp\left(\frac{\partial}{\partial s} G \frac{\partial}{\partial s}\right) \exp(-U^b[s]). \end{aligned} \quad (8)$$

Here we introduced the “bare” or initial local potential

$$U^b[s] = \sum_i u^b(s_i) \quad (9)$$

which will be renormalized by the RG procedure and in the LPA will remain local throughout the whole course of renormalization. Though from (8) it follows that  $u^b(x)$  in (9) formally contains a poorly defined contribution  $-\ln \delta(x^2 - 1)$ , this will not pose problems to us because, as shown in Appendix A, in the differential RG equation one can use  $\exp(-u^b)$  instead of  $u^b$  so in explicit calculations only the plain delta-function will appear.

As follows from (5), the spin correlation function can be found by differentiating the logarithm of  $Z[h]$  in (6) with respect to  $h_i$  twice which after setting  $h$  to zero gives in the matrix notation [7, 5, 6, 20]

$$\| \langle s_i s_j \rangle \| = G - G \frac{\partial^2 U[s]}{\partial s \partial s} G \Big|_{s=0}. \quad (10)$$

Because the exact partition function does not depend on  $r$ , the value of the latter can be chosen arbitrarily. In approximate calculations, however, the independence will usually be lost in which case  $r$  can be used as a free parameter to improve the approximation. In effective medium theories, such as CPA, one aims at choosing  $r$  in such a way that the second term in (10) disappeared and propagator  $G$  coincided with the exact correlation function. This would mean that the propagation of individual (quasi)particles within the medium is unperturbed by the scattering described by the second term, hence the term “effective medium”.

In general, however, it is impossible to set the second term in (10) to zero with the use of a single parameter because in this case  $r$  would coincide with the exact self-energy of the system which in non-trivial models depends on  $\mathbf{k}$ :  $r^{exact}(\mathbf{k})$ . With only one momentum-independent parameter at hand the effective medium condition can be satisfied only approximately. In the single-site approximation it is assumed that in the exact renormalized potential  $U^R[s] = -\ln R[s]$  (here and below we will designate by superscript  $R$  all fully renormalized quantities) the site-diagonal terms dominate so similar to (9)  $U^R$  can be approximated by a sum of local potentials  $u^R(x)$  and the condition

$$u_{xx}^R|_{x=0} = 0 \quad (11)$$

will nullify the second term in (10) locally which roughly corresponds to assuming the local self-energy  $r \approx r_{ii}^{exact}$ .

In studying the critical region one is interested mainly in the behaviour of the long range fluctuations, so with only one free parameter being available it seems more logical to impose the self-consistency condition on the self-energy at the smallest value of the momentum  $r \approx r^{exact}(\mathbf{k} \rightarrow \mathbf{0})$ . As will be shown below, in our SC RG approach this will amount to imposing condition (11) on the local potential  $u^R$  obtained as the solution of the LPA RG equation.

2.1. *The SC-LPA RG equation*

To find the partition function (6) it would be sufficient to calculate functional  $R$  in (8). But for our purposes will be sufficient to find only the function of the homogeneous field  $s_i = Const$  which in (6) will be replaced by  $Gh$ . Of course, before doing this substitution all partial derivatives in (8) should be taken.

Calculation of the derivatives in (8) by means of a RG technique in the LPA has been explained in detail in [10] (cf. our equation (8) with equation (4) in [10]). A slight difference with the present case is that in [10] all Fourier components  $s_{\mathbf{k}}$  were set to zero while we want to preserve the component with  $\mathbf{k} = \mathbf{0}$ . This is trivially achieved in equation (8) in [10] by simply not setting to zero the argument of the fully renormalized local potential  $u^R(x)$  because after successive elimination of all higher-momenta components the remaining  $x$  corresponds to  $s_{\mathbf{k}=\mathbf{0}}$  which we will set to zero only after using it, for example, in the calculation of the reduced free energy per site in the external homogeneous field  $h$  to be later used in the derivation of further thermodynamic quantities:

$$f(h) = -\ln Z = u^R(x)|_{x=h/r} - h^2/2r. \quad (12)$$

Here use has been made of equations (6), (7), (8) and (9).

More serious problem to resolve is that in [10] the RG equation was derived for statistical models in homogeneous space. Though it is not difficult to adopt the “layer cake” renormalization scheme of [10] to lattice models [20], in the present paper we adopt another possibility based on the observation made in [9] in the context of the CPA. Namely, in [9] it was shown that for any single-band DOS it is possible to construct rotationally-invariant dispersion  $\tilde{\epsilon}(k = |\mathbf{k}|)$  that would correspond to it. But in [22, 20] it was found that the LPA RG equations depend on the lattice structure only through the density of states (DOS) corresponding to dispersion  $\epsilon(\mathbf{k})$ . This means that it should be possible to apply to lattice systems the LPA equations derived for the homogeneous space. The only problem is that the isotropic dispersion is not uniquely defined [9]. However, as we show in Appendix A,  $\tilde{\epsilon}$  can be completely excluded from the LPA equation of [10] by a change of the evolution parameter from the momentum cut-off  $\Lambda$  to “time”  $t$  defined in (A.4) thus avoiding the ambiguity. Specifically, by substituting (A.3) and (A.8) in (A.1) one gets

$$u_t = \frac{1}{2} [p(t)u_{xx} - u_x^2]. \quad (13)$$

where the subscripts denote the partial derivatives and

$$p(t) = D_{tot}(t^{-1} - r) = \int_0^{t^{-1}-r} dE D(E) \quad (14)$$

in complete agreement with  $n = 1$  lattice case [20]. Note that in the ferromagnetic case under consideration the integration over  $t$  in (13) is bounded from above because  $D(E)$  in (14) vanishes at negative  $E$  where positive dispersion  $\epsilon(\mathbf{k})$  is equal to zero so when  $t$  exceeds  $r^{-1}$   $p(t)$  also turns to zero. Thus, unlike

in more conventional LPA approaches [11, 31] in [10] and in the SC LPA the evolution spans a finite interval of  $t$  values except at the critical point where  $t_{max} = r^{-1}$  becomes infinite.

Equation (13) with the initial condition (A.13) and the self-consistency condition (11) constitute the SC-LPA RG scheme that will be used in explicit calculations throughout the present paper.

The LPA equation (13) could be readily integrated numerically in the symmetric phase above  $T_c$ . Below  $T_c$ , however, insurmountable numerical difficulties have been encountered. The problem has been attributed to the exact quadratic partial solution (the Gaussian model) which in the coexistence region below  $T_c$  becomes negative and singular at some point  $t_{sing} > 0$ :

$$u^G(x, t) = \frac{x^2}{2(t - t_{sing})} + (\text{f.i.t.}) \quad (15)$$

where by (f.i.t.) we denoted field- or  $x$ -independent terms. At  $t = 0$  the initial curvature in solution (15) is negative and diverges to  $-\infty$  as  $t \rightarrow t_{sing}$ . The integration cannot go beyond this point because the singularity is non-integrable, so it was identified with the end point of the integration  $t_{sing} = 1/r$ . The singularity, however, is not a deficiency of the LPA. In fact, it ought to be expected on physical grounds because the magnetic susceptibility should be infinite in the coexistence region but according to (5) and (12) it is given by the second derivative

$$\chi = d^2 \ln Z / dh^2|_{h=0} = 1/r - u_{xx}^R|_{h=0}/r^2. \quad (16)$$

And because  $r$  in (16) is proportional to the squared inverse correlation length  $r \propto \xi^{-2}$  it is finite both above and below  $T_c$ . Hence, the infinite susceptibility can arise only from the second term, so its unboundedness is dictated by the physics of the problem.

The physical soundness of the approximation is gratifying but we have to find a way of dealing with the singularity. In view of the direct connection between  $u$  and the free energy (12), a plausible idea would be to resort to a Legendre transform (LT) of  $u(x)$ , say,  $v(y)$ , because under the transform the second derivatives of  $v$  and  $u$  would be inversely proportional to each other [23] and the infinity in  $u_{xx}$  would turn into numerically manageable zero in  $v_{yy}$ . This general idea is realized below in a non-canonical way via a LT-like  $t$ -dependent transform explained in Appendix B which for simplicity we will continue to call the LT transform. Equations (B.1) and (B.2) have been obtained as a generalization of the  $t$ -independent LT suggested in [24] (see also [11]). Though our LT does not have the canonical form [23], it solves the singularity problem because the transformed LPA equation

$$v_t = \frac{p(t)v_{yy}}{2(1 + \bar{t}v_{yy})} \quad (17)$$

( $\bar{t} = t - t_0$ ) obtained from (B.4) and (B.5) has a Gaussian solution with a  $t$ -independent quadratic in  $y$  term which thus is non-singular in  $t$ . In the coex-

istence phase where  $t_{sing} = 1/r$  the LT-transformed (15) reads

$$v_G(y, t) = -\frac{y^2}{2\bar{t}^R} + (\text{f.i.t.}) \quad (18)$$

where  $\bar{t}^R = 1/r - t_0$ . With the use of (B.5) susceptibility (16) expressed in the  $v - y$  variables is

$$\chi = \frac{1}{r} - \frac{v_{yy}^R}{r^2(1 + \bar{t}^R v_{yy}^R)} \Big|_{h=0}. \quad (19)$$

As is seen, though the solution (18) in the coexistent region is finite, the susceptibility in (19) is infinite, as needed.

It is to be noted that (15) and (18) are only particular solutions of the RG equations and there is no obvious reason why they should dominate the solution for arbitrary non-Gaussian models, especially taking into account that in the disordered phase the solution  $u$  or  $v$  for the IM are non-Gaussian. Nevertheless, in the numerical solutions of the IM in the coexistence region the  $y$ -dependent part of  $v^R$  was indistinguishable from  $v^G$  within the accuracy of the calculations which was  $O(10^{-6})$  in our case (see Appendix C). This is illustrated in figure C.7.

A minor inconvenience of dealing with the LT variables is that  $v$  and  $y$  do not have an obvious physical meaning. But in view of (B.3) the transform can be easily inverted, so that at the end of the integration we have

$$x = h/r = y + \bar{t}^R v_y^R \quad (20)$$

$$u^R = v^R + \bar{t}^R v_y^2/2. \quad (21)$$

Thus, in view of (12) both the field and the free energy can be represented in parametric form in terms of  $y$  and  $v$  so other thermodynamic quantities can be expressed through  $y$  and  $v$  with the use of the standard thermodynamic relations.

The discussion of the LPA solution below  $T_c$  will be continued in section 4 below but first we consider the simpler disordered phase.

### 3. Disordered phase

Using the IM language, in experiments above  $T_c$  in [18] the authors measured the spin-spin correlation function and compared it with that calculated in [16] for the nn bcc IM. In slightly modified notation ( $a_1$  instead of  $a$ ), expression (11.1) for the susceptibility in [16] reads

$$\hat{\chi}(\mathbf{k}, T) = \frac{(a_1/r_1)^{2-\eta}}{[(\kappa_1 a_1)^2 + a_1^2 K^2(\mathbf{k})/(1 - \eta/2)]^{1-\eta/2}}. \quad (22)$$

Definitions of quantities entering this expression can be found in [16] so here we only note that  $\kappa_1$  is the inverse correlation length  $\xi^{-1}$  and that  $r_1$  in (22) is unrelated neither to our  $r$  nor to the nn sites.



Table 1: Comparison of the parameters entering expressions (26) and (27) for nn Ising model on bcc lattice as calculated in the present work and in [16] (tables VI and VII). For simplicity, all numbers were rounded so as that the discrepancy between the two approaches were in one significant figure.

	$\nu$	$B_0$	$B_1$	$\eta$	$(r_1/a_1)_c$	$c$	$(a_1/r_1)_c^{2-\eta}$
LPA	0.65	0.352	-0.3	0	0.46	0.50	4.75
[16]	0.64	0.351	-0.1	0.06	0.45	0.47	4.77

In the LPA the susceptibility is given by  $G(\mathbf{k})$  (7) which, in particular, means that  $\eta = 0$  [11, 10] and in this approximation it should coincide with (22). To cast the two expressions in the same form we first multiply the numerator and the denominator of (7) by  $a_1^2$  and note that  $K^2(\mathbf{k})$  in (22) was defined in [16] as our  $\epsilon(\mathbf{k})$  but normalized so that at small  $k$  it behaved as  $k^2$  with the coefficient unity. In view of (4) this means that (7) will acquire the form of (22) if we further divide the numerator and denominator by  $(V_1 - V_2)a^2/k_B T$ . By comparing the numerators one finds that in the LPA:

$$\left(\frac{a_1}{r_1}\right)^2 \simeq \frac{3k_B T}{V_1 - V_2} = \frac{3T^r}{4(1 - V_2/V_1)} \quad (23)$$

where use has been made of the fact that  $(a_1/a)^2 = 3$  and for simplicity we introduced the reduced (dimensionless) temperature

$$T^r = \epsilon_1^{-1} = (V_1/4k_B T)^{-1}. \quad (24)$$

Similar comparison of the first terms in the denominators gives

$$(\kappa_1 a_1)^2 = (a_1/\xi)^2 \simeq 3T^d r/4(1 - V_1/V_2). \quad (25)$$

The values of the quantities in (22) were given by expressions (9.9) and (9.14) in [16]:

$$\log_{10} \kappa_1 a_1 \simeq \nu \log_{10} \tau + B_0 + B_1 \tau \quad (26)$$

and

$$r_1(T)/a_1 = (r_1/a_1)_c(1 - c\tau + \dots), \quad (27)$$

respectively, where  $\tau = |1 - T/T_c|$  and other parameters listed in tables VI and VII in [16].

For quantitative comparison, the SC-LPA equation (17) was solved numerically for nn bcc IM in the vicinity of  $T_c$  in the disordered phase. Details of the numerical techniques used are given in Appendix A. The results are compared with the solution of [16] in figure 1 and in table 1. As is seen, the largest discrepancy is between the values of  $B_1$ . But because in (26)  $B_1$  is multiplied by  $\tau$ , at the largest value of  $\tau$  in Fig. 1 it introduces the error amounting to only about 1% of  $B_0$ . As a result, in this range the discrepancy between the LPA values of  $\xi$  and the values calculated on the basis of (26) with the parameters from Table VI in [16] is smaller than 3%. When  $\tau \rightarrow 0$  the error becomes negligible so the discrepancy seen in the figure at small  $\tau$  should be attributed to the

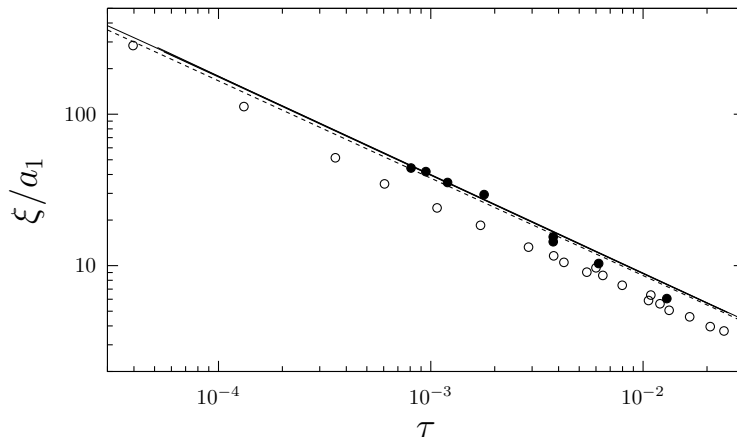


Figure 1: Correlation length above  $T_c$ : dashed curve and the empty circles were calculated as  $(\kappa_1 a_1)^{-1}$  on the basis of (26) with the parameters from [16] and from the experimental data of Fig. 10 in [18], respectively; three overlapping solid lines are the LPA solutions for the nn IM and for the IM with  $V_1 = 3.8$  mRy and two second neighbour interactions  $V_2 = 0.9$  mRy [19] and -1 mRy; the black circles are experimental data from Fig. 9 in [18].

difference  $\nu$ , as can be seen from a steeper LPA curve. Thus, with the overall discrepancy in a few percent the agreement can be deemed to be satisfactory taking into account that the authors assess the accuracy of (22) in 12% [16]. Besides, the LPA  $T_c^r$  agreed with the best known estimates for  $T_c$  in the nn bcc IM within 0.3% [20].

It is reasonable to assume that the accuracy of the LPA similar to the nn case will also hold for IM with not too large second neighbour interactions. This is further confirmed by the fact that  $T_c \simeq 748.5$  K calculated with the *ab initio* values of the interactions taken from Fig. 1 in [19]  $V_1 = 3.8$  mRy and  $V_2 = 0.9$  mRy differed from the experimental value 739 K only on 1.3%, especially taking into account that the neglected further neighbour interactions neglected in [19] due to their smallness may be responsible for the disagreement. The correlation length calculated with these parameters is also shown in figure 1 and is almost indistinguishable from the nn case. This means that according to our calculations the model can describe the experimental data in disordered phase as well as the nn model but, in addition it can predict  $T_c$  with reasonable accuracy and, besides, has a firm *ab initio* foundation [19].

To complete the check on the influence of the next neighbour interactions on the behaviour of the correlation length, a model with negative  $V_2$  was solved and also did not show appreciable deviations from the nn case. Thus, our calculations do not support the suggestion made in [25] that farther-neighbour interactions can be responsible for disagreement of the nn model with experimental data.

#### 4. Ordered phase

The behaviour of the order parameter below  $T_c$  measured in  $\beta$ -brass in [18] is more difficult to interpret quantitatively. Theoretically, in a close vicinity of the critical point the order parameter follows the power law

$$m_0^*(\tau) = a_0^* \tau^{\beta^*}, \quad (28)$$

where the order parameter  $m_0$ , the amplitude  $a_0$  and the critical exponent  $\beta$  have been starred for the reasons explained below. In the Ising universality class the order-disorder transitions are described by the universal critical order parameter exponent which value rounded to three significant digits is [27]

$$\beta \simeq 0.327 \quad (29)$$

where the last digit may be equal to 6 but the first and the second digits are considered to be firmly established. In this paper we will neglect distinctions between the true universal value (29), the value  $\beta$  found in [15] and  $\beta^{LPA} = 0.325$  because their differences are negligible on the scale of variation of  $\beta^*$  in our calculations below and in [18] where (28) fitted to experimental data in two temperature intervals gave the following numbers

$$\begin{aligned} \beta^* &= 0.313, & \tau &\lesssim 0.014 \\ \beta^* &= 0.29 \pm 0.01, & \tau &\lesssim 0.04 \end{aligned} \quad (30)$$

which disagree with (29) in the second and even in the first significant digit. Moreover, (30) and (30) violate the scaling relation  $\beta = \nu(1 + \eta)/2$  holding in 3D [27] because with  $\nu = 0.64$  adopted in [18]  $\beta^*$  should exceed 0.32 for any  $\eta > 0$ .

In principle, the discrepancies are not unexpected because the power laws with the universal exponents are strictly valid only asymptotically when  $\tau \rightarrow 0$  and cannot describe data on finite temperature intervals where the true behaviour is different and is unknown in 3D. Rigorous RG theory predicts an infinite number of correction terms of the power-law type with known exponents but not amplitudes [26]. Thus, expression (28) is not valid on any finite temperature interval and the quantities entering it do not have much physical meaning so they were marked by the stars to distinguish them from the physical spontaneous magnetisation  $m_0$ , the critical amplitude  $a_0$  and the universal critical exponent  $\beta$  that will be calculated below with the use of the SC-LPA RG equation.

Nevertheless, because in [18] some experimental data were fitted to (28), below we discuss peculiarities of such a fit with the reservation that fitting to an incorrect expression is a poorly defined problem and the fit results will depend on practically all details of the fitting procedure, such as the distribution of the measured points, their weights, etc. The main goal pursued by the nonperturbative RG approach is to calculate all quantities of interest directly without the need to resort to heuristic expressions of unknown validity.

As explained in Appendix C, below  $T_c$  two quantities should be determined self-consistently within the SC LPA approach: self-energy  $r$  and the spontaneous magnetisation  $m_0$ . With known  $v^R(y)$  the latter according to (5), (12), (B.3) and (21) can be calculated as

$$m_0 = y_0 - t_0 v_y^R|_{y_0} = y_0 / (1 - r t_0) \quad (31)$$

where the last equality was obtained from the Gaussian solution (18). In our calculations the Gaussian solution (18) agreed with the numerically obtained one within the accuracy of the calculations. But if in more accurate calculations the Gaussian solution will be found to be only approximate, the first equation in (31) should be used instead.

Because the phases above and below  $T_c$  are physically quite different, in the absence of quantitative criteria of the accuracy of the approach the SC-LPA solution should also be checked in the ordered phase by comparing it with reliable reference data. The highly accurate MC simulations in the ordered phase made in [15] perfectly suit this purpose. Though the model studied was the mn sc IM, similar to bcc the sc lattice is bipartite and its coordination is only 25% smaller so the accuracy of LPA in this system should be similar to what can be expected in the bcc case.

#### 4.1. Ordering on the sc lattice

The results of the MC simulations in [15] were summarized in the form of an interpolation formula

$$m_0(\tau) = \tau^\beta (a_0 - a_1 \tau^\theta - a_2 \tau) \quad (32)$$

where the precise parameter values are given in [15]; the rounded values can be found in table 2 below. In figure 2 magnetisation (32) is compared with the LPA calculations. The accuracy of expression (32) is quite high, of order of  $10^{-5}$  [15] but the accuracy of the LPA calculations were at best  $2 \cdot 10^{-3}$  at  $m_0 = 1$  because of the finite differentiation step used. Therefore, in all our fits and figures the smallest  $m_0$  was chosen to be 0.2 in order to have the accuracy at least not worse than 1%, though the LPA equation could be easily solved for much smaller magnetisations. Good accuracy of the data, however, is vital for our purposes because we intend to study quantitatively the deviations of the LPA data from the linearity in the region  $\tau \leq 0.04$  where they are hardly discernible on the scale of the graph in figure 2. The non-linearity of the logarithm of  $m_0(\tau)$  is, however, obvious from the fitting expression (32). To assess the quality of the LPA solution it was fitted to the LPA points in figure 2 with the use of the LPA order parameter exponent  $\beta = 0.325$  and the leading correction exponent taken to be  $\theta = 0.5$  [26] because the corrections to it are of higher order in  $\varepsilon = 4 - d$  ( $d$  the space dimensionality) than the LPA which is accurate only to the first order in  $\varepsilon$  [11, 10]. As can be seen from table 2, similar to the disordered case the worst agreement is with a correction term, this time with  $a_1$  which is about one third smaller than the MC value. Still, the largest error in  $m_0$  introduced

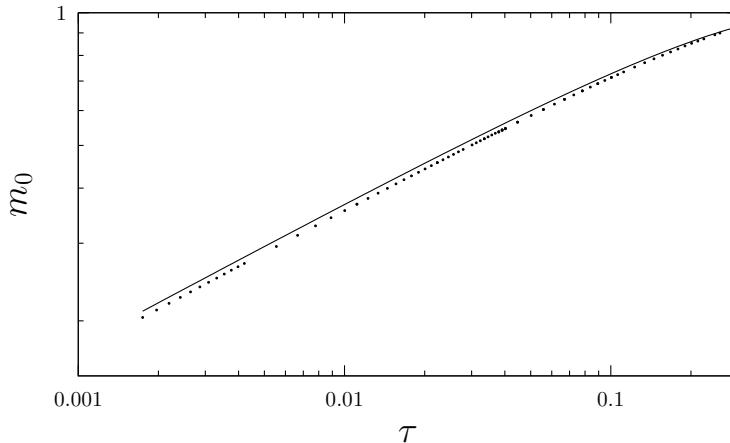


Figure 2: Spontaneous magnetisation in the sc IM: solid line—the interpolation of the exact MC simulations (32) [15], symbols—the LPA solution.

Table 2: Parameters of the LPA  $m_0(\tau)$  fit to (32) with  $\beta$  and  $\theta$  held fixed compared to rounded values from [15].

	$T_c$	$\beta$	$\theta$	$a_0$	$a_1$	$a_2$
LPA	4.475	0.325	0.50	1.62	0.22	0.41
[15]	4.512	0.327	0.51	1.69	0.34	0.43

by this discrepancy is about 3.6% at the maximum value of  $\tau = 0.26$ . It is even smaller at 0.04 and shrinks to zero as  $\tau \rightarrow 0$ . This, however, is an important difference to us because of the strong influence of the leading correction on the effective order parameter exponent  $\beta^*$  [27].

In [18], however, the data were fitted not to (32) but to more conventional power law (28) so let us find out how accurately the SC-LPA reproduces such fits. As was already pointed out, in the fit to an incorrect function all details of the fitting procedure may influence the results. Therefore, because in [18] the authors fitted a quantity proportional to  $m_0^2$ , in checking the reliability of SC-LPA we fitted the squared power law (28) to the squared MC data (32) by minimizing the integral

$$I = \int_{\tau_0}^{\tau} [m_0^*(\tau')^2 - m_0(\tau')^2]^2 d\tau' \quad (33)$$

with respect to  $a_0^*$  and  $\beta^*$ . In (33) it is implicitly assumed that all data have the same weight and, besides, are homogeneously distributed within the interval  $[\tau_0, \tau]$ . These assumptions, of course, are rather arbitrary but they will allow us to roughly estimate the span of variation of possible values of  $\beta^*$ .

The integrals in (33) can be calculated analytically and the parameters found exactly. The fitted values of  $\beta^*$  are shown in figure 3 by the solid lines. The upper line corresponds to the fit when the lower limit of integration in (33) was

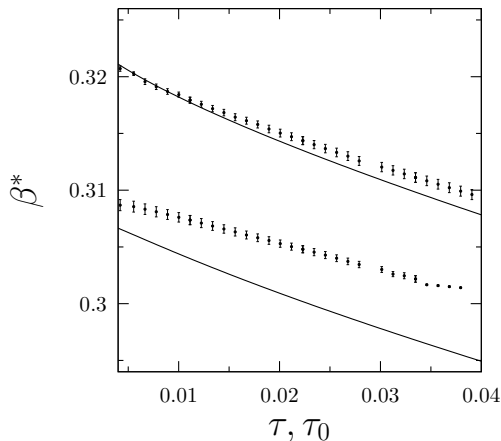


Figure 3: The effective order parameter exponent  $\beta^*$  fitted to the MC (solid lines) and to the LPA (symbols) simulation data. For details of the fitting procedure see the text.

held fixed at  $\tau_0^{min}$  corresponding to  $m_0 = 0.2$  while the upper limit varied from  $\tau_0$  to  $\tau^{max} = 0.04$ . At the lower line the upper limit was fixed while  $\tau_0$  varied from  $\tau_0^{min}$  to  $\tau^{max}$ . This case roughly imitates the situation when the data at small  $m_0$  are given very low weight because of larger errors.

Similar procedure was applied to the LPA data except that instead of the integral the sum over discrete points was used in the expression for  $I$ . As can be seen in figure 3, the agreement with the fit to MC data is not perfect and the LPA values show smaller deviations from the universal  $\beta$ . This reflects the smaller amplitude of the leading correction  $a_1$  noted above. But it should be born in mind that the deviation of  $\beta^*$  from  $\beta$  that we are interested in is less than 10% and in the worst case of agreement the LPA still predicts  $\sim 80\%$  of it. The important conclusion from these fits is that the deviations are similar in magnitude to those obtained experimentally and so potentially may explain them if the bcc case exhibits deviations of similar magnitude.

#### 4.2. Ordering on bcc lattice.

Thus, judging from the sc IM, the accuracy  $\sim 20\%$  may be expected in the LPA calculations of the effective exponent  $\beta^*$  in the bcc case shown in figure 4. The simulations were carried out for the same models as in section 3 but this time the difference between the three cases was clearly visible, though it was not large.

The important observation that can be made from figure 4 is that the fits seem to support the *ab initio* model of [19] in comparison with the nn IM ( $V_2 = 0$ ) used in the interpretation of experimental results in [18]. The difference between the two cases, however, is rather small, not exceeding the LPA errors estimated in the sc case so the question arises of whether the difference is real. Because the observation is one of the main results of the present study, below

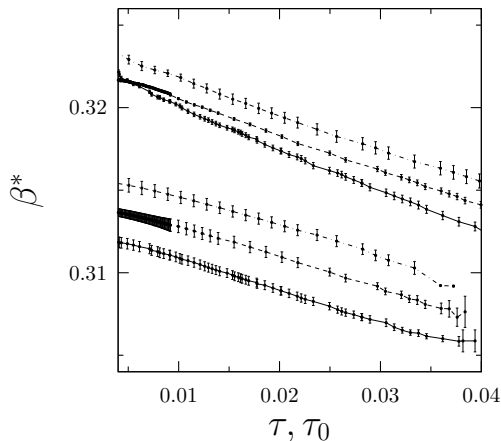


Figure 4: The upper and the lower groups of curves were obtained in as in figure 3. The simulated models were the same as listed in the caption to figure 1; the solid line corresponds to  $V_2 = 0.9$  mRy, dashed line to  $V_2 = 0$  and dashed-dotted line to  $V_2 = -1$  mRy.

are given qualitative arguments in favour of the conclusion that  $\beta^*(V_2 > 0)$  should indeed be smaller than  $\beta^*(V_2 = 0)$ .

To begin with, let us consider a FM IM with interactions of the form

$$\epsilon_{i \neq j} = C(\lambda)e^{-|i-j|/\lambda} \quad (34)$$

where  $|i - j|$  is the Euclidean distance between the sites,  $\lambda$  is a characteristic interaction range and  $C < 0$  can be chosen so as to keep the critical temperature fixed, though the latter is not obligatory. It is important to note that the nn IM belongs to the class of models (34) with  $\lambda \rightarrow 0$ . As is known, in the limit  $\lambda \rightarrow \infty$  model (34) tends to the exactly solvable mean-field (MF) model with all  $\epsilon_{i \neq j}$  being equal and the critical exponent  $\beta_{MF} = 0.5$ . The latter, however, holds only when  $\lambda = \infty$ . At any finite  $\lambda$  the model belongs to the same Ising universality class as the nn IM but as  $\lambda$  grows the true critical region shrinks and outside of it the MF behaviour dominates. Thus, when fitted to the power law (28) within a finite temperature interval the effective  $\beta^*$  should grow from its initial value close to 0.3 corresponding to nn IM (see figure 4 toward the MF value 0.5).

Model (34) is of interest to us because our model with  $V_2 = -1$  mRy can be accurately represented by (34). Indeed, with  $|V_2/V_1| \approx 0.26$  and the distances between the second and the first neighbours differing on  $\simeq 0.27a$ , the effective interaction range can be found to be  $\lambda \simeq 0.2a$ . The third neighbour interaction in this case according to (34) has the strength  $\sim 1.6\%$  of  $V_2$  so to a good approximation  $V_{i \geq 3}$  can be neglected. Obviously, the models with negative  $V_2$  but with smaller  $|V_2|$  can be approximated by (34) even better. Now, because in the short-range FM models belonging to the Ising universality class, there is no other critical or otherwise singular points, so it should be expected that the behaviour of  $\beta^*(\lambda)$  would be monotonous with larger  $\lambda$  meaning larger  $\beta^*$ .

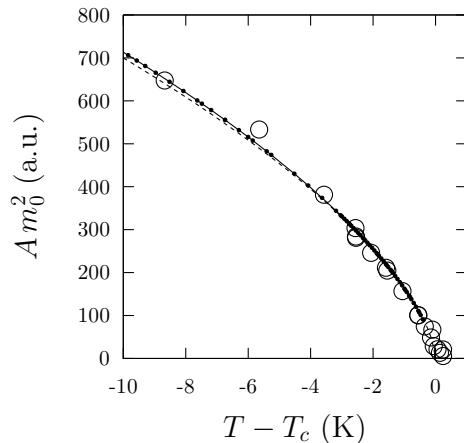


Figure 5: The empty circles and the dashed curve are, respectively, the experimental data and their power-law fit (28) with  $\beta^* = 0.313$  taken from Fig. 6 in [18]. The black dots (connected by solid line for better visibility) are the LPA results adjusted to the data via parameter  $A$ .

Thus we have shown that for a finite temperature interval near  $T_c$  and the models with only nn and the second neighbour interactions the effective order parameter exponent fitted at this interval should monotonously diminish from the value  $\beta^*(V_2 = -1 \text{ mRy})$  toward  $\beta^*(V_2 = 0)$ . Now by continuity arguments it can be concluded that when  $V_2$  grows farther by acquiring positive values the decrease of  $\beta^*$  should persist which qualitatively agrees with the fits shown in figure 4. Of course, if  $V_2$  becomes sufficiently large to cause the frustration effects the continuity may fail. But  $V_2 = 0.9 \text{ mRy}$  is rather small in comparison with  $V_1 = 3.8 \text{ mRy}$  so the continuity arguments should hold.

#### 4.3. Ordering in $\beta$ -brass.

The values of fitted  $\beta^*$  shown in figure 4 indicate that the experimentally observed behaviour of the order parameter for  $\tau \lesssim 0.014$  interpolated in [18] by the power law (28) with  $\beta^* = 0.313$  should be amenable to description by the SC-LPA equation with the *ab initio* parameters  $V_1$  and  $V_2$  as in [19]. Indeed, as shown in figure 5, in this region the LPA calculations compare well with the experimental points and the power law curve from [18]. This, however, does not mean that both descriptions are equally adequate. In contrast to the phenomenological theory of [18], in the RG approach the problems with the universality and the scaling relations do not arise [21, 27] and the LPA preserves these features, though with approximate values of critical exponents ( $\beta^{LPA} = 0.325$  and  $\nu^{LPA} = 0.65$ ) [11, 10, 31]. The small deviations from the best known values are expected to be corrected in the future with the use of techniques developed in the theory of nonperturbative RG [12]. Our use of the rotationally-invariant formalism to describe lattice models should considerably facilitate the task. But the main advantage of the SC-LPA is that there is



no need in heuristic expressions to fit experimental data because all observable quantities can be calculated directly.

Farther from  $T_c$ , however, in the interval  $\tau \lesssim 0.04$  the experimentally found value  $\beta^* = 0.29 \pm 0.01$  can hardly be reproduced in the LPA because the effective beta range in figure 4 extends from  $\sim 0.305$  upwards. The LPA values of  $m_0^2$  calculated at the seven  $\tau$  points close to those in the inset in Fig. 11 in [18] fitted to the power law (28) have given  $\beta^* \approx 0.315 \pm 0.002$  which is noticeably greater than (30). Because LPA overestimates  $\beta^*$ , the real discrepancy may be smaller but if the sc case is representative of what may be expected on the bcc lattice, the downward shift of  $\beta^*$  in figure 3) would be too small to explain the remaining discrepancy  $\Delta\beta = 0.025$ .

Thus, the value of effective  $\beta^* = 0.29$  cannot be quantitatively understood within the model with parameters of [19]. Two possible explanations for this failure can be envisaged. First, at  $\tau = 0.04$  the calculated long range order parameter reaches as large value as 0.53 which may influence the interatomic interactions propagated via the electronic subsystem and thus change the values of  $V_1$  and  $V_2$  as well as introduce additional effective cluster interactions.

The explanation may also lie in the experimental uncertainties in the temperature measurement in [18] which according to the authors were of the order of 0.2 K. To assess possible implications, let us assume that away from  $T_c$  the measured temperatures were systematically overestimated so that they were effectively shifted toward the critical temperature being about  $\Delta T \approx 0.2$  K closer to  $T_c$  than they were in reality. Alternatively, this may be a consequence of the error in determination of  $T_c$ , or errors of both kinds could contribute to the shift. Now by fitting the same seven LPA points as above to the re-defined  $\tau = 1 - (T + \Delta T)/T_c$  in (28) one finds  $\beta^* = 0.302 \pm 0.005$  which already overlaps with (30). Taking into account that LPA overestimates the effective exponents the agreement with experiment may be even better. As can be seen in figure 6, qualitatively the fit looks as good as the corresponding fit in [18] except at the point closest to  $T_c$ . But this point is one of the many in the vicinity of  $T_c$  which are rather scattered due to the steepness of the order parameter in this region and the perfect agreement of the point with the fitting curve could be accidental.

## 5. Conclusion

In this paper a SC RG equation in the LPA has been derived and used in a quantitative description of experimental data on the ordering in  $\beta$ -brass [18]. It has been shown that with the use of the *ab initio* values of the effective pair interactions [19] it may be possible to calculate within the SC-LPA the critical temperature  $T_c$  with  $\sim 1\%$  accuracy and provide a description of the critical behaviour in the 1.4% vicinity of  $T_c$  satisfying the universality principle and the scaling relations between the critical exponents. These features were lacking in the phenomenological theory in [18] which was based on the approximate solution of the nn IM [16]. To validate the SC-LPA it has been applied to the

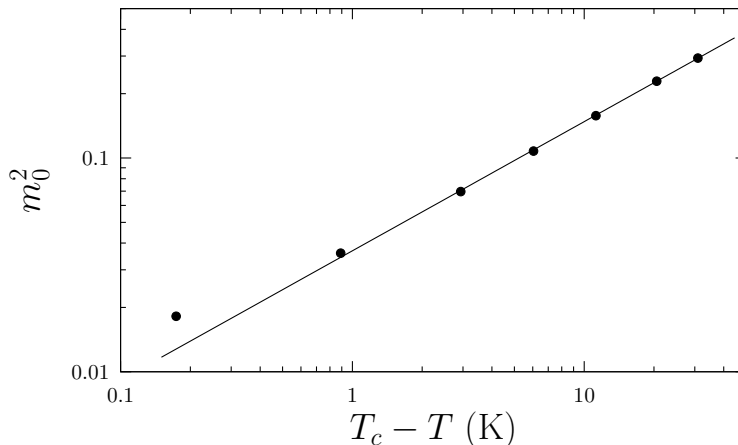


Figure 6: LPA data points (symbols) shifted on  $\simeq 0.2$  K toward  $T_c$  fitted to power law (28) (solid line) with  $\beta^* \simeq 0.30$ ; experimental points at these temperatures were fitted in [18] with  $\beta^* \simeq 0.29 \pm 0.01$ .

sc and the bcc nn IMs and agreement within a few-percent accuracy has been found with existing theoretical calculations [15, 16].

In the sc case it has been found that in the SC-LPA the order parameter is accurately described within the distance  $\sim 25\%$  away from  $T_c$ . Therefore, the inability of the theory to reproduce the observed  $\beta^*$  at the distance  $\sim 4\%$  from the critical point has led us to the conclusion that either the model parameters are strongly influenced by the order that may exceed the value 0.5 in this range or that the temperatures were systematically overestimated within the accuracy of the measurements  $\sim 0.2$  K or both possibilities contributed to the discrepancy. Further experimental and theoretical research would be needed to resolve these issues.

The most serious deficiency of the proposed approach is that it cannot be rigorously justified beyond the perturbation theory which is a common problem in all strongly coupled many-body and field-theoretic models. Strong coupling, however, is frequently encountered in physical systems which was the reason for the development of heuristic approaches to deal with it. Arguably, among lattice models the best known are the CPA and the DMFT (see the bibliography on these methods in review articles [1, 28]). It is remarkable that, as was shown in [7], these and some other strong coupling approximations can be derived within the same formalism and with the same self-consistency condition as that used in the present paper. This suggests that in approximations of this kind there exists some underlying mechanism of suppression of corrections to it. This assumption is supported by the excellent agreement of many experimental and MC data with the CPA [1, 13, 14] and with the SC-LPA [20]. Moreover, non-local corrections to the CPA in a strongly disordered tight-binding model alloy calculated in [29] were in excellent agreement with the exact MC simulations, thus justifying and improving the CPA in this particular case. Finally, cluster generalizations of the

single-site theories have been actively developed and promising results obtained [5, 28, 6, 8]. So there is a good deal of hope that further research along these lines will make possible to set CPA-like approaches, including the SC-LPA, on a firm theoretical footing.

## Appendix A. LPA for lattice models

The LPA RG equation (13) in the main text can be obtained from the RG equation derived in [10] as follows. First, in the case of a one-component field corresponding to the IM equation (8) in [10] reads

$$\frac{\partial u}{\partial \Lambda} = \frac{1}{2} \frac{dG}{d\Lambda} \left[ \left( \frac{\Lambda}{\Lambda_{BZ}} \right)^3 \frac{\partial^2 u}{\partial x^2} - \left( \frac{\partial u}{\partial x} \right)^2 \right] \quad (\text{A.1})$$

where  $u$  is the local potential,  $\Lambda$  the momentum cut-off,  $x$  the local field and the propagator

$$G(\Lambda) = \frac{1}{c(\Lambda)} = \frac{1}{\tilde{\epsilon}(\Lambda) + r}, \quad (\text{A.2})$$

where  $c$  is the coefficient of the quadratic in the field part of the Hamiltonian in [10] which for easier comparison with (7) is convenient to separate into the dispersion term  $\tilde{\epsilon}(\Lambda)$  behaving as  $\sim \Lambda^2$  when  $\Lambda \rightarrow 0$  and the momentum-independent self-energy  $r$ . Besides, we explicitly included in (A.1) the maximum cut-off momentum  $\Lambda_{BZ}$ , where  $BZ$  stands for the ‘‘Brillouin zone’’. In [10]  $\Lambda_{BZ}$  was set equal to unity but because in the present paper we want to apply the equation to arbitrary lattices, the size of BZ should also be arbitrary. Also, this factor corrects the equation from the dimensionalities standpoint.

By substituting (A.2) into (A.1) one obtains the equation that explicitly depends on the rotationally-invariant dispersion  $\tilde{\epsilon}(\Lambda)$  which according to [9] can be fitted to the DOS of a lattice model thus enabling application of (A.1) to lattice systems. In general the fit is not unique [9] but, fortunately, in the case of equation (A.1) this difficulty can be overcome by a change of the evolution variable. To show this let us first divide both sides of the equation by  $dG/d\Lambda$  and on the basis of definition

$$dt = \frac{dG}{d\Lambda} d\Lambda = dG \quad (\text{A.3})$$

introduce the new independent variable

$$t = G = \frac{1}{\tilde{\epsilon}(\Lambda) + r}. \quad (\text{A.4})$$

Because all quantities here are positive,  $t$  is bounded from above by the maximum value  $1/r$  reached when  $\tilde{\epsilon} = 0$ .

In (A.1)  $\Lambda$  is now a function of  $t$  which formally can be found from (A.4) as

$$\Lambda(t) = \tilde{\epsilon}^{-1}(t^{-1} - r) \quad (\text{A.5})$$

where  $\tilde{\epsilon}^{-1}$  is the function inverse to  $\tilde{\epsilon}(\Lambda)$ .

The explicit dependence of  $\Lambda$  in (A.1) on  $t$  can be found with the help of the integral

$$\Lambda^3(t) = \int_0^{\Lambda_{BZ}} k^3 \delta[\tilde{\epsilon}^{-1}(t^{-1} - r) - k] dk. \quad (\text{A.6})$$

which after integration by parts can be transformed to

$$\begin{aligned} \Lambda^3(t) &= 3 \int_0^{\Lambda_{BZ}} k^2 \theta[\tilde{\epsilon}^{-1}(t^{-1} - r) - k] dk \\ &= 3 \int_0^{\Lambda_{BZ}} \theta[t^{-1} - r - \tilde{\epsilon}(k)] k^2 dk, \end{aligned} \quad (\text{A.7})$$

where on the first line the boundary terms were omitted by assuming that the first term in the argument of  $\theta$ -function is smaller than  $\Lambda_{BZ}$  and on the second line we further assumed that  $\tilde{\epsilon}(k)$  is a monotonous function. Though the integrand in (A.7) is isotropic, it can be integrated over all three components of  $\mathbf{k}$  by considering  $\tilde{\epsilon}$  as a function of  $k = |\mathbf{k}|$ . Now the coefficient of the second derivative in (A.1) can be cast in the form convenient for generalization to the lattice case:

$$p(t) = \left( \frac{\Lambda(t)}{\Lambda_{BZ}} \right)^3 = \frac{1}{V_{BZ}} \int_{BZ} d\mathbf{k} \theta[E - \tilde{\epsilon}(\mathbf{k})] \Big|_{E=t^{-1}-r} \quad (\text{A.8})$$

where  $V_{BZ} = 4\pi\Lambda_{BZ}^3/3$ . As is easily seen, the last expression is just the integrated DOS of the quasiparticle band with dispersion  $\tilde{\epsilon}$ :

$$D_{int}(E) = \int_0^E D(E') dE' \quad (\text{A.9})$$

where  $D(E)$  is the DOS corresponding to  $\tilde{\epsilon}$  and, by construction, to  $\epsilon(\mathbf{k})$ . In this way  $\tilde{\epsilon}$  can be totally excluded from equation (A.1).

Thus, we have shown that the rotationally invariant  $G$  from [10] and our lattice  $G$  lead to the same LPA RG equation provided  $D(E)$  is the same. This makes possible to establish connection between the partition functions in both cases. By comparing our equations (6) and (8) with equation (4) in [10] for  $n = 1$  one sees that our  $U^b$  differs from  $H_I$  in [10] only in terms that are constant in the field and “time” variables. But the LPA equations depend only on the derivatives so the constant terms in the free energy are unchanged by the renormalization and can be accounted for at any stage. Below they will be gathered into one expression (A.13) to facilitate their analysis.

Incidentally, (A.8) is also valid for  $E > \max \tilde{\epsilon}$ , that is, above the upper edge of the DOS in which case the theta-function is equal to unity so the integrated DOS of a filled band is unity. The values of  $E$  in this range are needed to integrate the RG equation in the range where  $t$  in (A.4) changes from zero to the minimum value of  $G(\Lambda_{BZ} = 1)$  (see Fig. 1 in [10]):

$$0 \leq t \leq t_0 = \min_{\Lambda} G = (r + \max_{\Lambda} \tilde{\epsilon})^{-1} = [r + \max_{\mathbf{k}} \epsilon(\mathbf{k})]^{-1} \quad (\text{A.10})$$

Because  $p(t) = 1$  is constant in this range, substitution  $u = -\ln w$  reduces the RG equation to the diffusion equation which is integrated from  $t = 0$  to  $t_0$  with the use of the Gaussian diffusion kernel as

$$w(x, t_0) = (2\pi t_0)^{-1/2} \int dy e^{-(x-y)^2/2t_0} e^{-u^b(y)} \quad (\text{A.11})$$

This solution is particularly useful in the IM case where according to (8) and (9) the “bare” initial local potential

$$\exp[-u^b(x)] = \det(2\pi G)^{(1/2N)} e^{(r-\epsilon_0)/2} [\delta(x-1) + \delta(x+1)] \quad (\text{A.12})$$

is singular and difficult to deal with numerically. Substituting (A.12) in (A.11) one gets after some rearrangement

$$u(x, t_0) = \frac{x^2}{2t_0} - \ln \cosh \frac{x}{t_0} - \ln 2 + \frac{1}{2}(\epsilon_0 + \epsilon_{max}) + \frac{1}{2N} \ln \det \frac{r + \epsilon}{r + \epsilon_{max}} \quad (\text{A.13})$$

It is to be noted that because by assumption  $\tilde{\epsilon}(k)$  and  $\epsilon(\mathbf{k})$  have the same DOS, the maxima of both dispersions which define its upper edge should be the same by construction. Also, the same DOS means the same spectrum and the eigenvalues density which means the same determinants in both cases. So in the initial condition (A.13)  $\tilde{\epsilon}(k)$  can be replaced by its lattice homologue.

The usefulness of gathering all constants in  $u(x, t_0)$  can be seen from the fact that the integration range of the SC-LPA equation  $\bar{t}^R = 1/r - 1/(r + \epsilon_{max})$  scales as  $r^{-2}$  at large  $r$ , that is, in both limits  $T \rightarrow \infty$  and  $T \rightarrow 0$ . Which means that in these limits  $u(x, t_0) = u^R(x)$  so, for example, it is easy to see using (12) and (11) that in the  $T \rightarrow \infty$  limit the SC-LPA predicts the exact reduced free energy  $-\ln 2$ . Further, by using (12), (21) and (C.2) it can be shown that  $m_0 \rightarrow 1$  when  $T \rightarrow 0$ . Furthermore, at large  $r$  when the integration interval is small the SC-LPA equation can be integrated as a series in  $\bar{t}^R$  which can be further used to develop high- or low-temperature expansions of the solution for comparison with known results.

## Appendix B. The Legendre transform

### Appendix B.1. Regularization of equation (13)

To avoid dealing numerically with non-integrable singularity in the solution (15) of equation (13) it was found sufficient to slightly modify the Legendre transform for LPA equations suggested in [24] (see also [11]). The modification consists in introducing  $t$ -dependence into the transform as

$$v(y, t) = u(x, t) - \frac{1}{2} \bar{t} u_x^2 \quad (\text{B.1})$$

$$y(x, t) = x - \bar{t} u_x(x, t) \quad (\text{B.2})$$

where  $\bar{t} = t - t_0$  with  $t_0$  defined in (A.10). This choice was made for convenience and in general any constant can be used instead of  $t_0$ . The independent variables in (B.1) and (B.2) are  $x$  and  $t$ ,  $v$  and  $y$  being their functions.

Now by comparing equations (B.1) and (B.2) differentiated with respect to  $x$  it can be seen that

$$v_y = u_x \quad (\text{B.3})$$

if  $y_x \neq 0$ . Similarly, by differentiating the equations with respect to  $t$  one finds

$$v_t = u_t + \frac{1}{2}u_x^2 = \frac{1}{2}p(t)u_{xx} \quad (\text{B.4})$$

where the second equality follows from (13). Finally, differentiating (B.3) with respect to  $x$  and substituting  $y_x$  obtained from (B.2) one arrives at the relation

$$u_{xx} = \frac{v_{yy}}{1 + \bar{t}v_{yy}} \quad (\text{B.5})$$

which being substituted in (B.4) gives the transformed RG equation (17) in the main text.

### Appendix C. Numerical procedures

The evolution equation (17) has been solved by the method of lines with the use of LSODE routine [30] for 2500 discretization points at the positive (due to the symmetry)  $y$  axis. The point separation was  $\Delta y = 2 \cdot 10^{-3}$  which in [31] was shown to be already small enough to give accurate values of many quantities of interest. In the double precision code [30] the use of smaller  $\Delta y$  was plagued with instabilities which restricted the accuracy of calculations of  $m_0$  to  $O(\Delta y)$ . The second derivatives have been approximated by the three-term central differences in the LPA equation and by four-term one-sided differences at the points nearest to the jump in figure C.7 with the quadratic accuracy  $O(\Delta y^2) \sim O(10^{-6})$  in both cases. Similar calculations performed in [31] within different renormalization schemes with the use of a quadruple precision software showed that the accuracy can be considerably improved. Besides, in calculations of [31] the behaviour of the second derivative of the renormalized local potential qualitatively similar to that shown in figure C.7 was observed and its formal and physical features discussed in detail. In the present study we adopted the conclusion made in [31] that the discontinuity in the second derivative is physically correct and real, though a rigorous formal proof would be desirable.

The integrated DOS needed in  $p(t)$  has been calculated by numerical integration over BZ in (A.8) with  $\tilde{\epsilon}$  replaced by  $\epsilon(\mathbf{k})$ . The step size in the momentum integration was  $\sim 0.01$  ( $\pi/300$ ). The integration was performed twice with the integrand Fermi smeared at two small Fermi temperatures  $T_F$  and subsequently interpolated to  $T_F = 0$ . The integrations were performed at 300 energy points and spline-interpolated in between. To improve precision at the band edges the exactly known behaviour (4) was used. The accuracy of the approximations from the renormalization group standpoint has been checked by comparing the

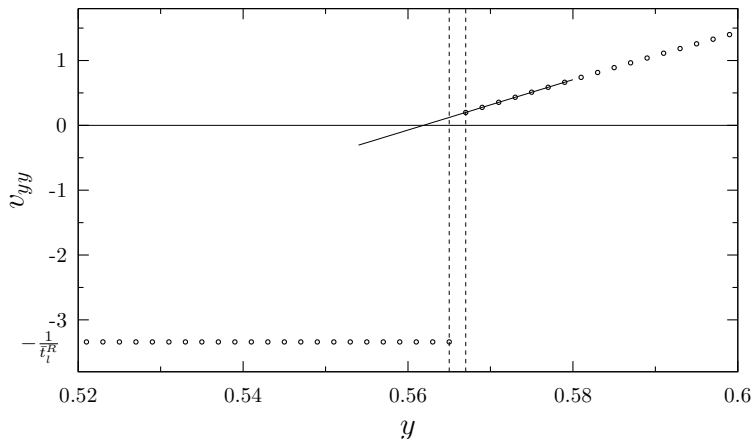


Figure C.7: Circles: the second derivative of  $v(y)$  calculated for the nn sc Ising model below  $T_c$  at an intermediate ( $l$ -th) iteration;  $\bar{t}_l^R = 1/r_l - 1/(r_l + \epsilon_{max})$ . As is seen, the derivative interpolated from the right of the jump interval bounded by vertical dashed lines does not turn to zero within the interval so further iterations are needed.

solutions of the LPA equation (17) obtained with the interpolated  $p(t)$  and with the accurate analytical interpolation given in [32]. No noticeable differences were found.

The solution proceeded iteratively with the self-consistent  $r$  obtained as the limit of the recursion

$$r_{l+1} = r_l + v_{yy}^R|_{x=0} \quad (\text{C.1})$$

which converged when the self-consistency condition

$$v_{yy}^R|_{h+=0} = 0 \quad (\text{C.2})$$

was satisfied. According to (B.5) this is equivalent to the self-consistency condition (11) with  $h$  in (C.2) expressed through  $y$  according to (21). In the symmetric phase this simply means  $y = 0$  but below  $T_c$  two stable solutions appear corresponding to  $y = \pm y_0 \neq 0$  with the spontaneous magnetisation  $m_0$  given by (31). So two conditions should be fulfilled below  $T_c$ : (C.2) and  $h = 0$ .

### Acknowledgements

I express my gratitude to Université de Strasbourg and IPCMS for their hospitality. I am indebted to Hugues Dreyssé for support and encouragement.

This research did not receive any specific grant from funding agencies in the public, commercial, or not-for-profit sectors.

## References

## References

- [1] R. J. Elliott, J. A. Krumhansl, P. L. Leath, The theory and properties of randomly disordered crystals and related physical systems, *Rev. Mod. Phys.* 46 (1974) 465–543.
- [2] J. Ziman, P. Ziman, *Models of Disorder: The Theoretical Physics of Homogeneously Disordered Systems*, Cambridge University Press, 1979.
- [3] F. Ducastelle, *Order and Phase Stability in Alloys*, North-Holland, Amsterdam, 1991.
- [4] A. Zunger, First-principles statistical mechanics of semiconductor alloys and intermetallic compounds, in: P. E. A. Turchi, A. Gonis (Eds.), *Statics and Dynamics of Alloy Phase Transformations*, Vol. 319 of NATO ASI Series B: Physics, Plenum Press, New York, 1994, pp. 361–419.
- [5] V. I. Tokar, A new cluster method in lattice statistics, *Comput. Mater. Sci.* 8 (1997) 8–15.
- [6] T. L. Tan, D. D. Johnson, Topologically correct phase boundaries and transition temperatures for Ising Hamiltonians via self-consistent coarse-grained cluster-lattice models, *Phys. Rev. B* 83 (2011) 144427.
- [7] V. I. Tokar, A new series expansion in lattice statistics, *Phys. Lett. A* 110 (1985) 453–456.
- [8] V. I. Tokar, Hybrid cluster+RG approach to the theory of phase transitions in strongly coupled Landau-Ginzburg-Wilson model (2016). [arXiv:1606.06987](https://arxiv.org/abs/1606.06987).
- [9] B. Velický, S. Kirkpatrick, H. Ehrenreich, Single-site approximations in the electronic theory of simple binary alloys, *Phys. Rev.* 175 (1968) 747–766.
- [10] V. I. Tokar, A new renormalization scheme in the Landau-Ginzburg-Wilson model, *Phys. Lett. A* 104 (1984) 135–139.
- [11] C. Bervillier, Revisiting the local potential approximation of the exact renormalization group equation, *Nucl. Phys. B* 876 (2013) 587.
- [12] J. Berges, N. Tetradis, C. Wetterich, Non-perturbative renormalization flow in quantum field theory and statistical physics, *Phys. Rep.* 363 (4) (2002) 223 – 386.
- [13] A. E. Kissavos, S. I. Simak, P. Olsson, L. Vitos, I. A. Abrikosov, Total energy calculations for systems with magnetic and chemical disorder, *Comput. Mater. Sci.* 35 (1) (2006) 1–5.



- [14] A. E. Kissavos, S. Shallicross, L. Kaufman, O. Grånäs, A. V. Ruban, I. A. Abrikosov, Thermodynamics of ordered and disordered phases in the binary Mo-Ru system, *Phys. Rev. B* 75 (18).
- [15] A. L. Talapov, H. W. J. Blöte, The magnetization of the 3d ising model, *J. Phys. A* 29 (1996) 5727.
- [16] M. E. Fisher, R. J. Burford, Theory of Critical-Point Scattering and Correlations. I. The Ising Model, *Phys. Rev.* 156 (1967) 583–622. doi:10.1103/PhysRev.156.583.
- [17] A. J. Liu, M. E. Fisher, The three-dimensional ising model revisited numerically, *Physica* 156A (1989) 35–76.
- [18] A. Madsen, J. Als-Nielsen, J. Hallmann, T. Roth, W. Lu, Critical behavior of the order-disorder phase transition in  $\beta$ -brass investigated by x-ray scattering, *Phys. Rev. B* 94 (2016) 014111. doi:10.1103/PhysRevB.94.014111.
- [19] P. E. A. Turchi, M. Sluiter, F. J. Pinski, D. D. Johnson, D. M. Nicholson, G. M. Stocks, J. B. Staunton, First-principles study of phase stability in Cu-Zn substitutional alloys, *Phys. Rev. Lett.* 67 (1991) 1779–1782.
- [20] V. I. Tokar, Effective medium approach in the renormalization group theory of phase transitions (2019). arXiv:1910.05123.
- [21] K. G. Wilson, J. Kogut, The renormalization group and the  $\epsilon$  expansion, *Phys. Rep.* 12 (1974) 75–199.
- [22] T. Machado, N. Dupuis, From local to critical fluctuations in lattice models: A nonperturbative renormalization-group approach, *Phys. Rev. E* 82 (2010) 041128. doi:10.1103/PhysRevE.82.041128.
- [23] R. K. P. Zia, E. F. Redish, S. R. McKay, Making sense of the legendre transform, *Am. J. Phys.* 77 (2009) 614–622.
- [24] T. Morris, Equivalence of local potential approximations, *J. High Energy Phys.* 0507 (2005) 027.
- [25] O. W. Dietrich, J. Als-Nielsen, Temperature Dependence of Short-Range Order in  $\beta$ -Brass, *Phys. Rev.* 153 (1967) 711–717. doi:10.1103/PhysRev.153.711.
- [26] F. J. Wegner, Corrections to Scaling Laws, *Phys. Rev. B* 5 (1972) 4529–4536. doi:10.1103/PhysRevB.5.4529.
- [27] A. Pelissetto, E. Vicari, Critical phenomena and renormalization-group theory, *Phys. Rep.* 368 (2002) 549–727.
- [28] T. Maier, M. Jarrell, T. Pruschke, M. H. Hettler, Quantum cluster theories, *Rev. Mod. Phys.* 77 (2005) 1027–1080.

- [29] V. I. Tokar, I. V. Masanskiy, Accounting for the short-range order in the electronic theory of disordered alloys, *Fiz. Metall. Metalloved.* 64 (1987) 1207–1211.
- [30] K. Radhakrishnan, A. C. Hindmarsh, Description and use of LSODE, the Livermore solver for ordinary differential equations, Tech. Rep. UCRL-ID-113855, LLNL (December 1993).
- [31] J.-M. Caillol, The non-perturbative renormalization group in the ordered phase, *Nucl. Phys. B* 855 (2012) 854–884.
- [32] R. J. Jelitto, The density of states of some simple excitations in solids, *J. Phys. Chem. Solids* 30 (3) (1969) 609–626.